

Cross-relaxation in dense ensembles of NV centers and application to magnetometry

Clément Pellet-Mary

PhD Defense



Université
de Paris



institut
universitaire
de France

Outline

Sensing with quantum mechanics

NV centers and diamonds in practice

Low field depolarization magnetometry (LFDM)

Depolarization mechanisms in dense NV ensemble

Outline

Sensing with quantum mechanics

NV centers and diamonds in practice

Low field depolarization magnetometry (LFDM)

Depolarization mechanisms in dense NV ensemble

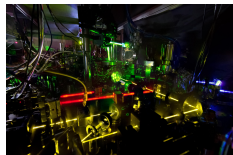
Quantum sensing and metrology

Quantum metrology:

Using quantum* properties to create more sensitive measurement protocols.

* quantum \equiv discrete energy levels

Time measurement



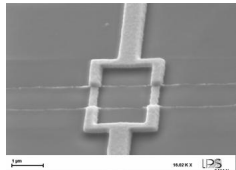
Atomic clock

Medical imaging



MRI

Magnetometry



SQUIDs

Magnetometry key parameters

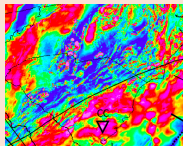
Magnetoencephalography



$$|\vec{B}| \sim 10 \text{ fT}$$

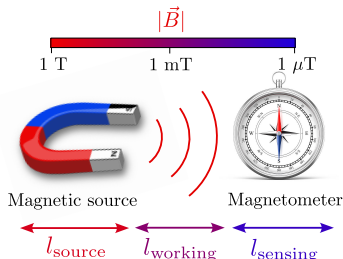
$$l \sim 1 \text{ cm}$$

Earth's magnetic field anomaly



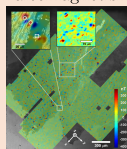
$$|\vec{B}| \sim 10 \text{ nT}$$

$$l \geq 1 \text{ km}$$



Optimum:
 $l_{\text{sensing}} \approx \max\{l_{\text{source}}, l_{\text{working}}\}$

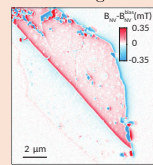
Paleomagnetism



$$|\vec{B}| \sim 100 \text{ nT}$$

$$l \sim 10 \mu\text{m}$$

Surface magnetism



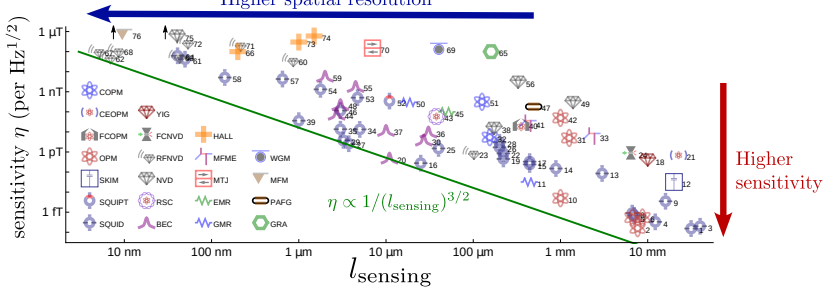
$$|\vec{B}| \sim 100 \mu\text{T}$$

$$l \sim 50 \text{ nm}$$

Sate of the art magnetometers

Mitchell, M. W., & Alvarez, S. P. *Reviews of Modern Physics*, 92(2), 021001.

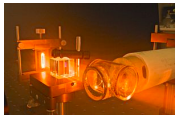
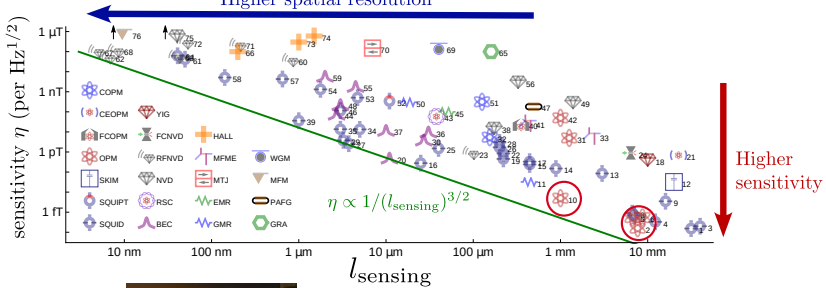
Higher spatial resolution



Sate of the art magnetometers

Mitchell, M. W., & Alvarez, S. P. *Reviews of Modern Physics*, 92(2), 021001.

Higher spatial resolution



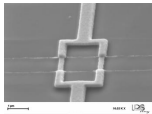
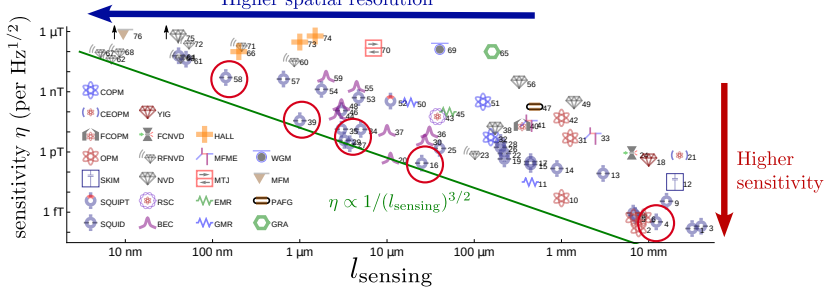
Optically pumped magnetometers (OPM)

Optically detected spin precession
of alkali vapor cell

Sate of the art magnetometers

Mitchell, M. W., & Alvarez, S. P. *Reviews of Modern Physics*, 92(2), 021001.

Higher spatial resolution



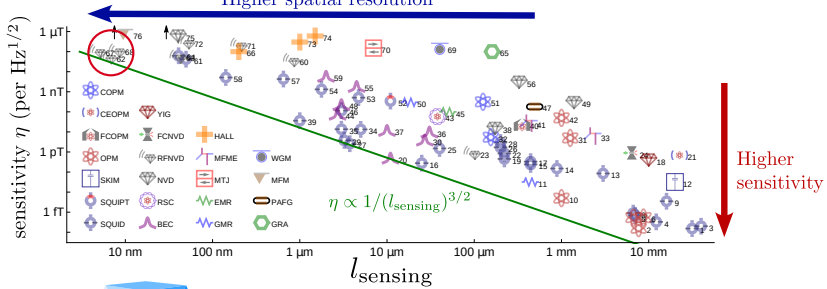
Superconducting quantum interference device (SQUID)

Magnetic field screening due to quantized magnetic flux

Sate of the art magnetometers

Mitchell, M. W., & Alvarez, S. P. *Reviews of Modern Physics*, 92(2), 021001.

Higher spatial resolution



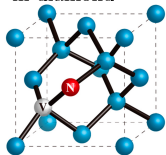
Nitrogen-Vacancy center in diamond (NV center)

Optically detected spin interferometry

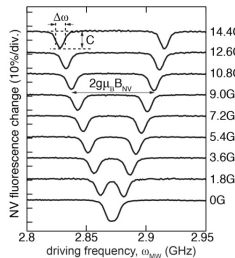
NV center overview

Rondin, L. et al. Reports on progress in physics, 77(5), 056503.

Point-like defect
in diamond



Electronic spin 1:
 \rightarrow 2 spin transitions



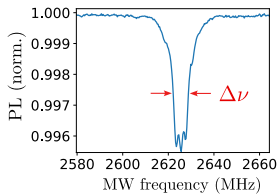
Zeeman effect:
 \rightarrow linear dependence of the spin transition frequency with \vec{B}

- Works at room temperature
 - Can be put arbitrarily close to the magnetic source
(low toxicity, chemically inert)
- \rightarrow Potential replacement for SQUID and OPM ?

NV center magnetometry sensitivity

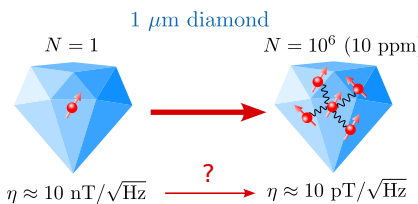
Ideal (DC) sensitivity for N independent NV centers:

$$\eta [T/\sqrt{\text{Hz}}] \approx \frac{\hbar \sqrt{\Delta\nu}}{g\mu_B C \sqrt{N}}$$

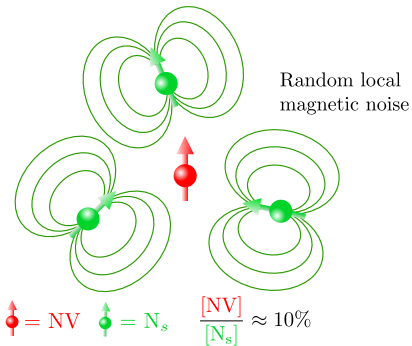


- \hbar : Planck constant
 - μ_B : Bohr magneton
 - g : NV electron Landé factor
 - C : Spin readout contrast
 - N : Number of NV centers
 - $\Delta\nu = \frac{1}{T_2^*}$: Spectral linewidth
- Constants

Experimental parameters
- Sample parameters

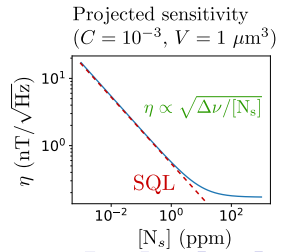
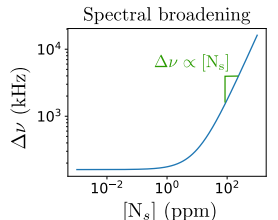


NV center magnetometry: the interaction limit



Going beyond the “Interaction limit” ($[\text{N}_s] > 10 \text{ ppm}$):

- Decoupling interaction (Hamiltonian engineering)
- Exploiting interactions



Sensing with quantum mechanics

NV centers and diamonds in practice

Low field depolarization magnetometry (LFDM)

Depolarization mechanisms in dense NV ensemble

Diamond properties

NV center energy levels

Basic experiment with NV centers

Outline

Sensing with quantum mechanics

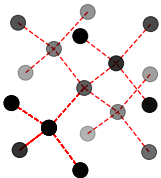
NV centers and diamonds in practice

Low field depolarization magnetometry (LFDM)

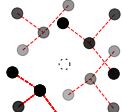
Depolarization mechanisms in dense NV ensemble

Colored centers in diamond

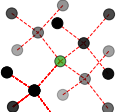
Diamond crystal lattice



Point-like defects

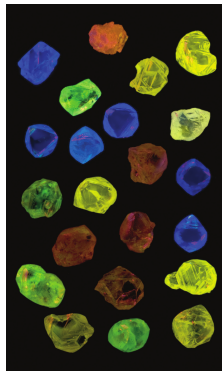
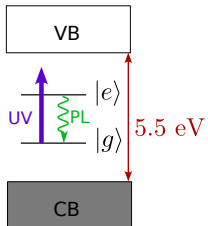


Vacancy



Substitution

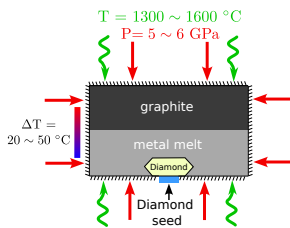
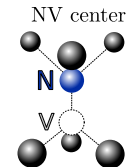
Colored center fluorescence



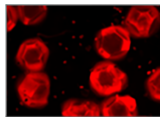
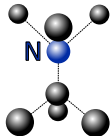
Natural diamonds fluorescence under UV light

Synthetic diamond and NV centers

High Pressure High Temperature
(HPHT)

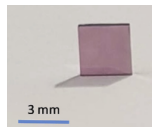
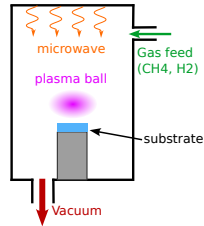


N_s (P1 center)



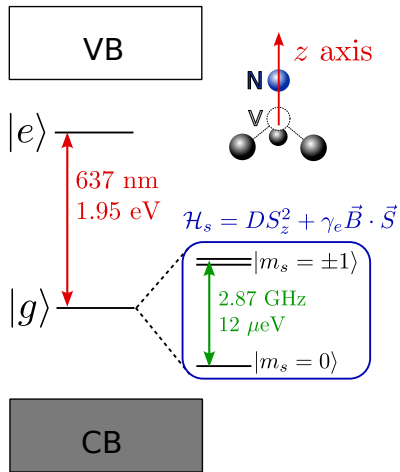
Adamas 15/150 μm
 $[N_s] \approx 100 \text{ ppm}$
 $[NV] \approx 3 \text{ ppm}$

Chemical Vapour Deposition
(CVD)

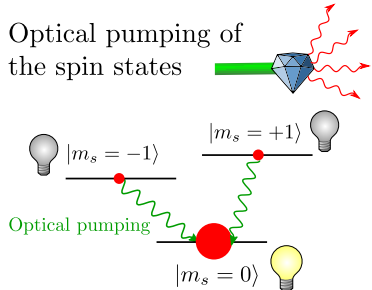
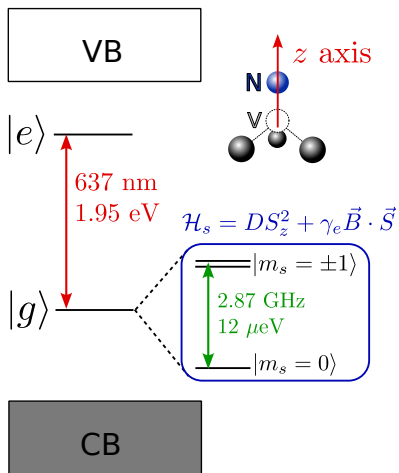


IRCP-LSPM
 $[N_s] \approx 25 \text{ ppm}$
 $[NV] \approx 4.5 \text{ ppm}$

The NV center energy levels

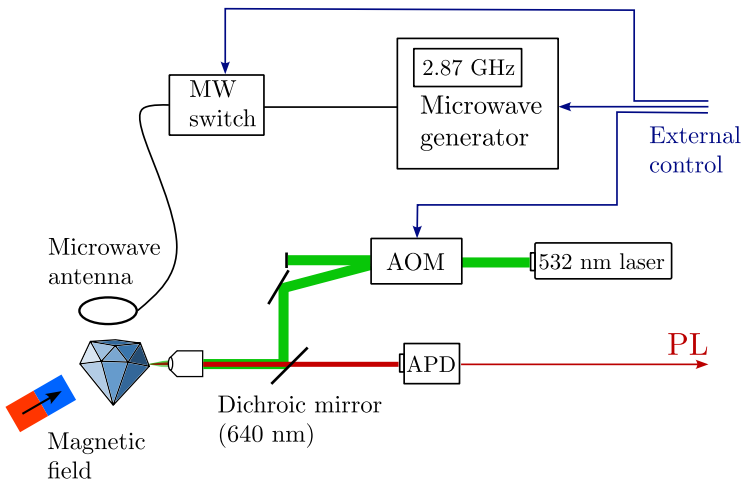


The NV center energy levels

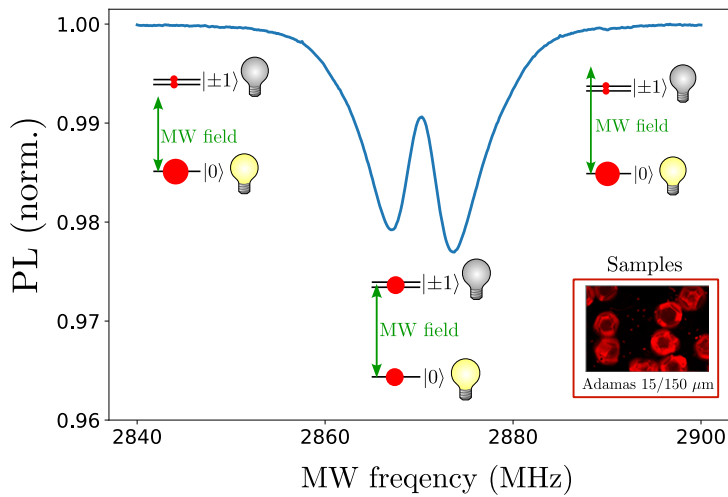


- Population accumulation in the $|0\rangle$ state
 - ↳ Initialization of the spin state
- $|0\rangle$ state brighter than $|\pm 1\rangle$ states
 - ↳ Optical readout of the spin state

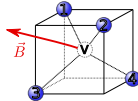
Experimental setup



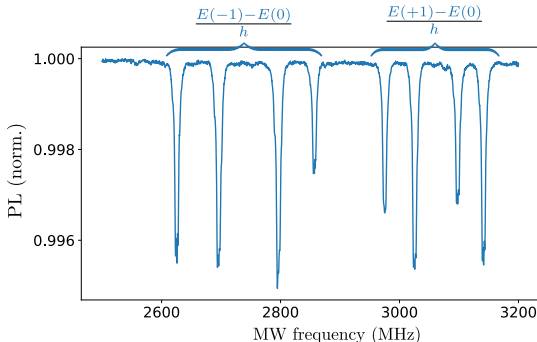
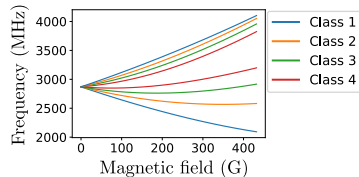
Optically detected magnetic resonance (ODMR)



ODMR with NV ensemble: the 4 classes



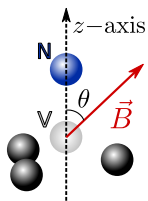
4 different projections of \vec{B}
over the 4 possible NV axes
 \rightarrow 4 classes of resonances



Transverse magnetic field effect

$$\hat{\mathcal{H}}_s = D S_z^2 + \gamma \mathbf{B} \cdot \hat{\mathbf{S}}$$

$$D = 2.87 \text{ GHz}, \gamma = 2.8 \text{ MHz/G}$$

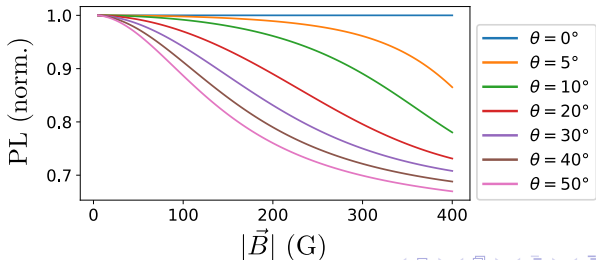


$$\mathcal{H}_s = \begin{pmatrix} | -1 \rangle & | 0 \rangle & | +1 \rangle \\ D - \gamma B_z & \gamma B_{\perp} & 0 \\ \gamma B_{\perp} & 0 & \gamma B_{\perp} \\ 0 & \gamma B_{\perp} & D + \gamma B_z \end{pmatrix}$$

When $D \gg \gamma B_{\perp}$:

- (Red circle) = Zeeman shift
- (Green oval) = State mixing

$$B_z = |\vec{B}| \cos \theta \quad B_{\perp} = |\vec{B}| \sin \theta / \sqrt{2}$$



Outline

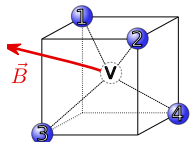
Sensing with quantum mechanics

NV centers and diamonds in practice

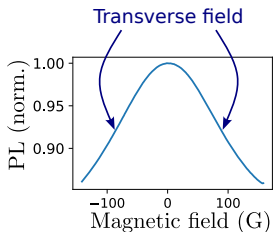
Low field depolarization magnetometry (LFDM)

Depolarization mechanisms in dense NV ensemble

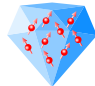
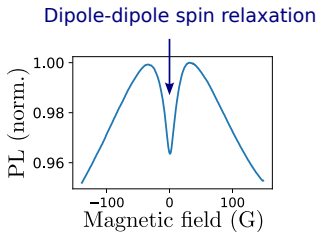
Depolarization of dense NV ensemble at low magnetic field



Non-zero transverse
magnetic field
on all 4 classes



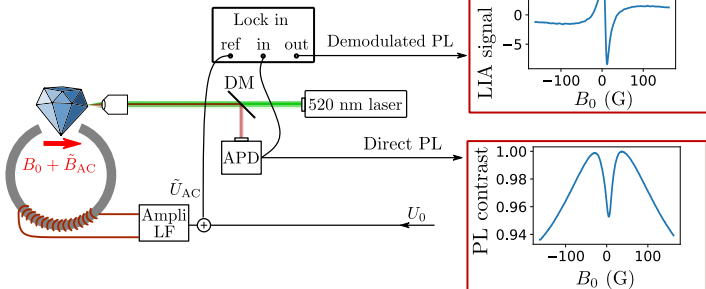
Low NV density
 $[NV] \leq 100$ ppb



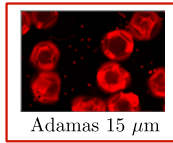
High NV density
 $[NV] \geq 1$ ppm

LFDM experimental setup

Experimental setup



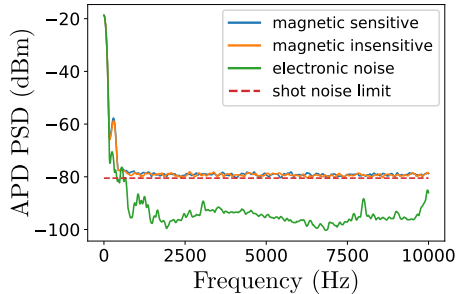
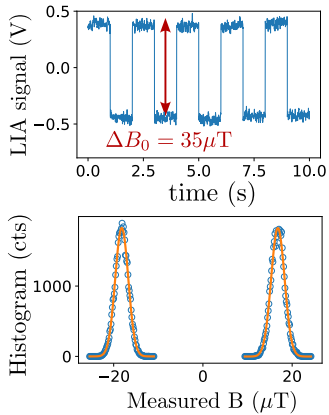
Samples



Experimental parameters

- $f_{\text{mod}} \sim 1 \text{ kHz}$
- $|B_{\text{mod}}| \sim 10 \text{ G}$
- $I_{\text{las}} \sim 1 \text{ mW}$
- $\text{PL} \sim 1 \mu\text{W}$

Sensitivity of LFDM



Shot noise limited for $f_{\text{mod}} > 500 \text{ Hz}$

$$\text{Low pass filter } \tau = 3 \text{ ms} \quad \sqrt{\langle \delta B^2 \rangle} \approx 1.2 \mu\text{T}$$

$$\rightarrow \text{sensitivity } \eta = \sqrt{2\tau \langle \delta B^2 \rangle} \approx 116 \text{ nT}/\sqrt{\text{Hz}}$$

Comparison with the state of the art

Sensitivity comparison

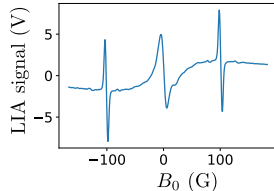
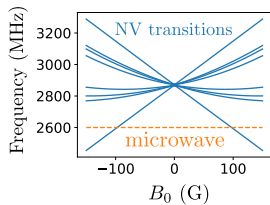
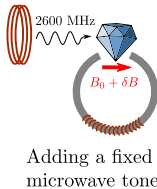
	GSLAC [1]	ODMR [2]	LFDM
η (nT/ $\sqrt{\text{Hz}}$)	0.3*	0.015	116
V (μm^3)	??	$5.2 \cdot 10^6$	$3.3 \cdot 10^3$
η_v (nT $\mu\text{m}^{3/2}\text{Hz}^{-1/2}$)	??	34	6700

[1] Zheng, H.[...] Budker, D. (2020). Physical Review Applied, 13(4), 044023.

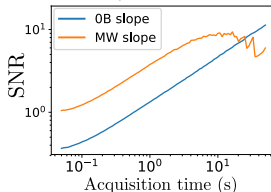
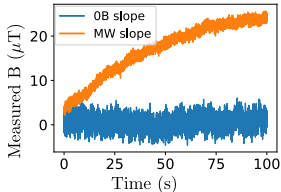
[2] Barry, J. F. [...] Walsworth, R. L (2016). PNAS, 113(49), 14133-14138.

	ODMR	GSLAC	LFDM
Microwave free	✗	✓	✓
Low magnetic field (<10 G)	✓	✗	✓
Robust to T° and B-field inhomogeneities	✗	✗	✓
Orientation free (polycrystalline, powder)	✗	✗	✓

Comparison with CW ODMR



Temporal stability

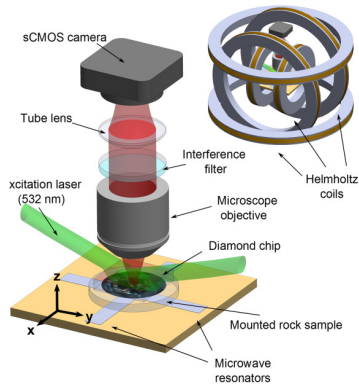
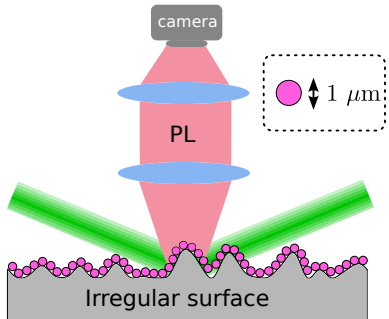


$$\text{MW slope sensitivity: } \eta \approx 40 \text{ nT}/\sqrt{\text{Hz}}$$

$$B=0 \text{ sensitivity: } \eta \approx 120 \text{ nT}/\sqrt{\text{Hz}}$$

Application: wide-field magnetometry on irregular surfaces

(Commercially available $1 \mu\text{m}$ diamonds)



Glenn, D. R. [...] Walsworth, R. L. (2017)
Geochemistry, Geophysics, Geosystems, 18(8), 3254-3267.

Area normalized sensitivity:
 $\eta_S \approx 6 \mu\text{T} \cdot \mu\text{m}/\sqrt{\text{Hz}}$

Area normalized sensitivity:
 $\eta_S \approx 20 \mu\text{T} \cdot \mu\text{m}/\sqrt{\text{Hz}}$

Outline

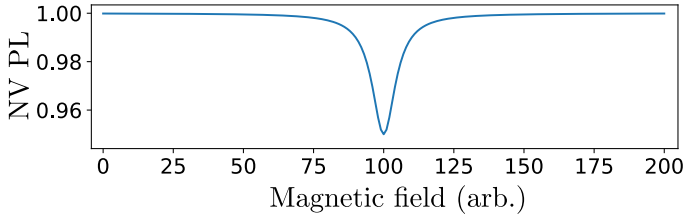
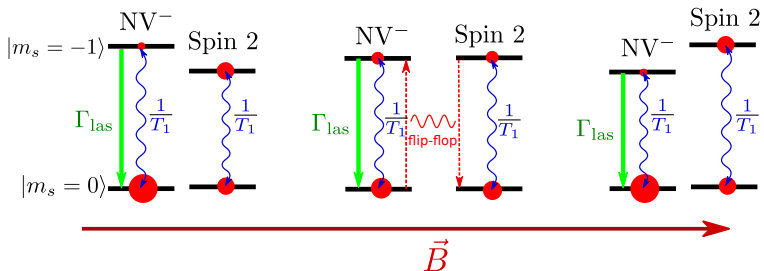
Sensing with quantum mechanics

NV centers and diamonds in practice

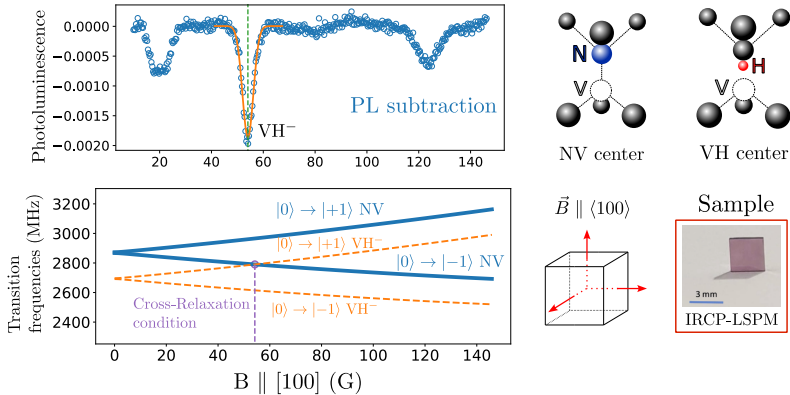
Low field depolarization magnetometry (LFDM)

Depolarization mechanisms in dense NV ensemble

Principle of cross-relaxation with NV centers



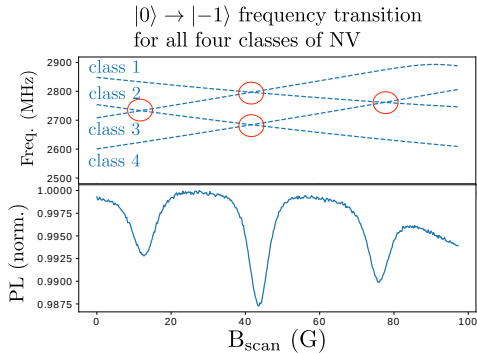
Example: Cross-relaxation between NV centers and VH⁻



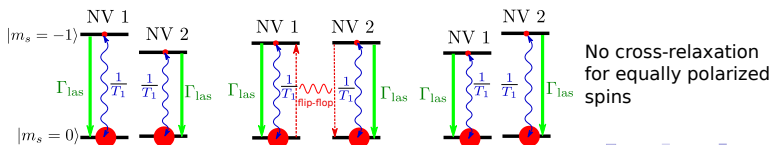
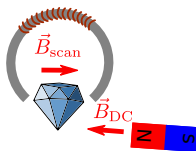
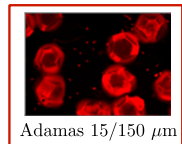
Optical detection of paramagnetic defects in diamond grown by chemical vapor deposition

C. Pellet-Mary, P. Huillery, M. Perdriat, A. Tallaire, and G. Hétet
 Phys. Rev. B **103**, L100411 – Published 24 March 2021

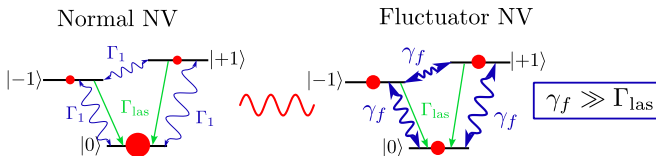
Cross-relaxation between NV centers and NV centers



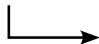
Sample



Presentation of the fluctuator model



Fluctuators are NV centers with a fast intrinsic depolarization mechanism



Localized noise sources with the spectral response of an NV center

Precedents in:

- P-doped Si
- solid-state NMR
- FRET

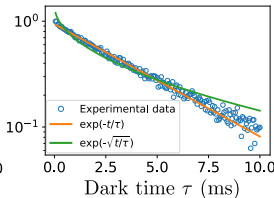
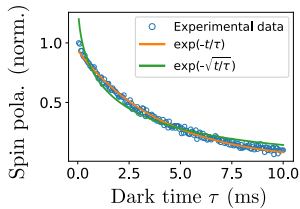
Possible microscopic explanation:

- charge tunneling
- modulation of J-coupling

Up to 1/3 of all NV centers could be fluctuators

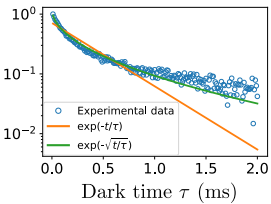
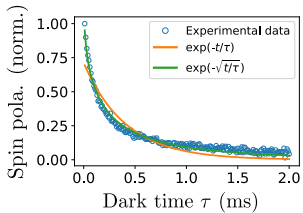
Choi, Joonhee, et al. Physical review letters 118.9 (2017): 093601.

Stretched exponential decay profile



Low NV density

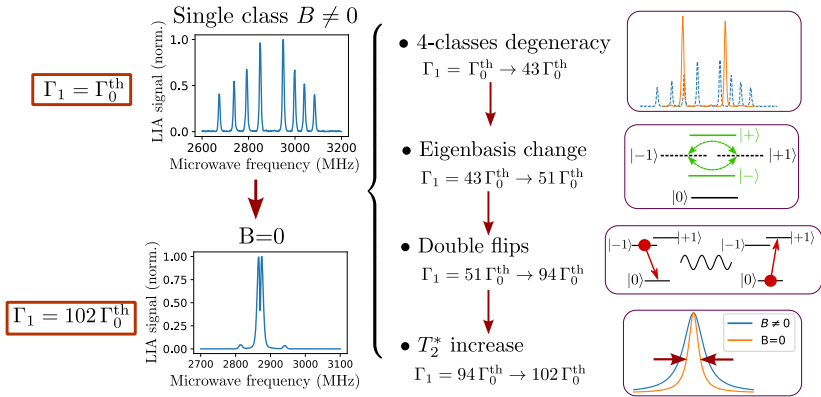
- Exponential profile
- $T_1 \sim 5$ ms



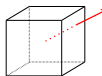
High NV density

- Stretched exp. profile
- $T_1 \sim 0.5$ ms

Zero field depolarization sources (theory)

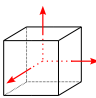
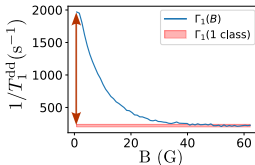


Summary of the experimental observations



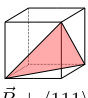
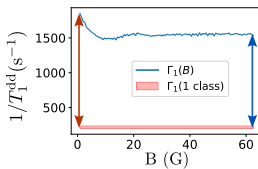
Random \vec{B}

- 4-classes degeneracy
- Eigenbasis change
- Double-flips
- T_2^* change



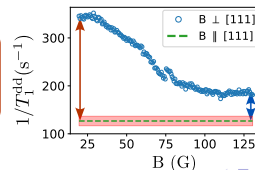
$\vec{B} \parallel \langle 100 \rangle$

- 4-classes degeneracy
- Eigenbasis change
- Double-flips
- T_2^* change



$\vec{B} \perp \langle 111 \rangle$

- 4-classes degeneracy
- Eigenbasis change
- Double-flips
- T_2^* change

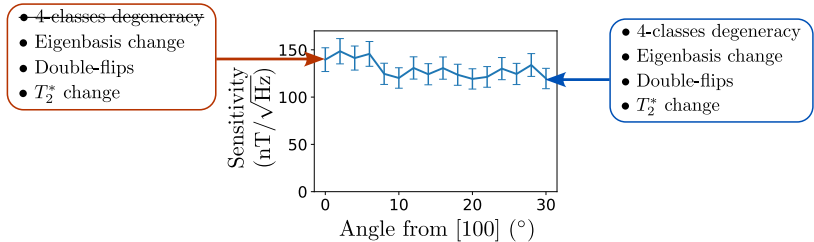
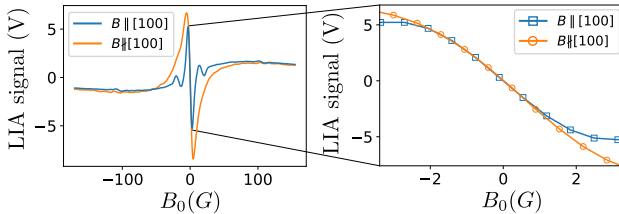


- 4-classes degeneracy
- Eigenbasis change
- Double-flips
- T_2^* change

- 4-classes degeneracy
- Eigenbasis change
- Double-flips
- T_2^* change

- 4-classes degeneracy
- Eigenbasis change
- Double-flips
- T_2^* change

Angular sensitivity of LFDM

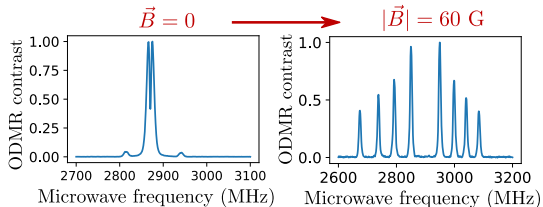


The 4-classes degeneracy is not the limiting factor of the sensitivity

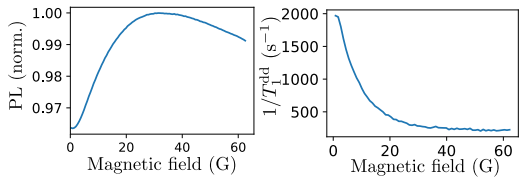
Conclusion

Acknowledgments

Experiment: \vec{B} in arbitrary direction

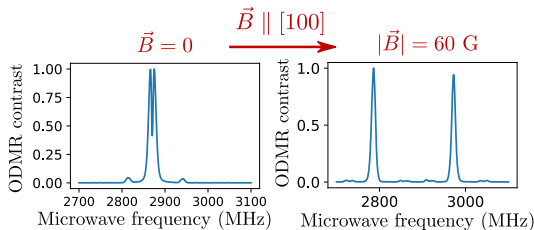


- 4-classes degeneracy
- Eigenbasis change
- Double-flips
- T_2^* change

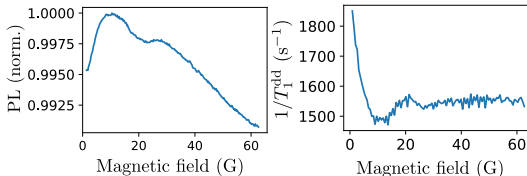


$\Gamma_1(B = 0) \approx 10 \Gamma_1(B \neq 0)$
 $\sim 4\%$ PL contrast
HWHM ~ 9 G

Experiment: $\vec{B} \parallel [100]$



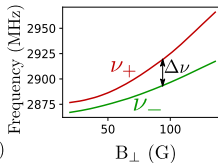
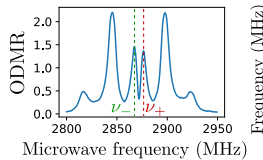
- 4-classes degeneracy
- Eigenbasis change
- Double-flips
- T_2^* change



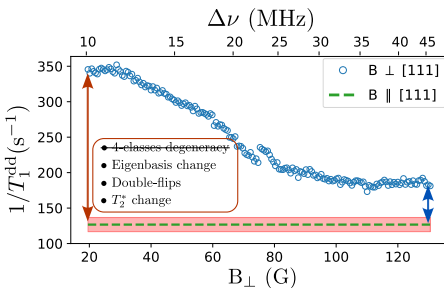
$\Gamma_1(B = 0) \approx 1.2 \Gamma_1(B \neq 0)$
 $\sim 0.5\%$ PL contrast
HWHM ~ 2 G

Classes degeneracy is the dominant cause of depolarization at low magnetic field

Experiment: $\vec{B} \perp [111]$



Same eigenbasis :
 $|\pm\rangle = \frac{|+1\rangle \pm |-1\rangle}{\sqrt{2}}$
 for $\vec{B} \perp [111]$ than for $\vec{B} = 0$



canceling out double flips
 with transverse field

Double flips are the second dominant cause
 of depolarization at low magnetic field